2 x 1 Rectangular-Patch Antenna Array at 2.4 GHz

JEANETTE MEJIA ROJAS[1], MARIO REYES-AYALA[1],
EDGAR ALEJANDRO ANDRADE-GONZALEZ[1], SANDRA CHAVEZ-SANCHEZ[2], HILARIO TERRES-PEÑA[2], RENE RODRIGUEZ-RIVERA[2]
[1]Department of Electronics, [2]Department of Energy
Metropolitan Autonomous University
San Pablo 180, Col. Reynosa Tamaulipas, Azcapotzalco (ZIP 02200), Mexico City
MEXICO

Abstract: - In this paper a microstrip antenna array is carried out. The array has two rectangular patches in a linear 2 x 1 array. This work includes the design, simulation, implementation and evaluation of both, a single radiator and the linear two rectangular microstrip antenna array. The antenna array was designed and built for low-cost and noncomplex manufacturing techniques, because the array is dedicated for educational purposes in under-graduate radiocommunication courses at Metropolitan Autonomous University. The mechanical tolerance in the structure dimensions is around 0.2 mm, that is easy to be obtained by an inexpensive CNC or very well-known optical techniques. The simulation and optimization of the array was computed using HFSS and the results of this stage include antenna patterns and the reflection coefficient (S11). Besides, the experimental evaluation of the array is quite similar to the simulations results in both, radiation patterns and the frequency response using the matching interval, for a single radiator and the 2x1 array.

Key-Words: - Array antenna, microstrip, rectangular patch, reflection coefficient, antenna pattern, antenna bandwidth, matching network, return loss.

Received: May 23, 2022. Revised: March 9, 2023. Accepted: April 20, 2023. Published: May 8, 2023.

1 Introduction

Many modern radio-communication systems use array antennas, due to some important advantages. Cellular and broadcasting communication systems have coverage areas that can be changed over time. In this scenario, a flexible antenna pattern is more practical with a single-radiator antenna [1], [2]. The power of a single element of a antenna array can be multiplied by a factor. The antenna array sums the single radiators contributions in a vectorial result. If the coverage area is changing, the radiation pattern of the array can be adjusted manually or employing a control system. The time used in a new setup configuration is narrowed down significantly and can be modified dynamically in more complex systems [2], [3], [4].

Antenna arrays can also identify the direction of several sources in space with the aim to improve the quality of service in Personal Communication System (PCS). As a example of this, 4G and 5G uses 2D and 3D spatial discrimination, by using planar and tri-dimensional antenna arrays in the base stations. Moreover, the channel capacity can be increased using these types of antennas [1]. [2], [3], [6], [7].

The microstrip radiator was selected as a single radiator in the array, because it is compatible with planar surfaces and it has low-cost implementation. The rectangular microstrip is one of the simplest geometries and is normally presented in radiocommunication and antenna under-graduate courses. A small set of variables are involved in rectangular, circular and triangular geometries if are chosen for the patch of the single-radiator.

2 Antenna Array design

The design of the antenna array is divided into two parts, single or primary radiator and the 2x1 array including the matching network.

2.1 Primary radiator design

A rectangular microstrip antenna can be approximate using the Munson procedure, that has been improved and expanded over the years. In this method, the patch radiator is modeled by a microstrip transmission line, that normally needs a matching technique, see Fig. 1. Other matching techniques uses LCR circuits or shunt stubes implemented by transmission lines [5], [6], [7], [8], [9], [10], [11].

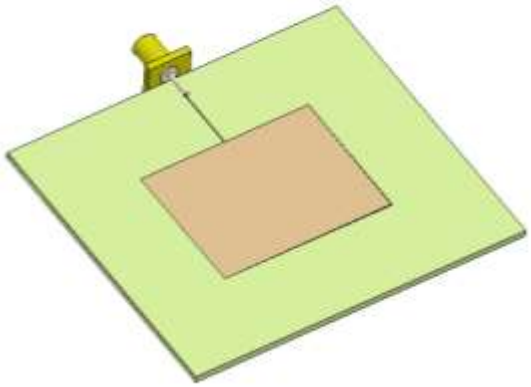

Fig.1 Geometry of rectangular patch antenna.

The design procedure begins with the width of the patch in the top layer of the Printed Circuit Board (PCB), see equation (1).

$$W = \frac{1}{2f_r\sqrt{\mu_0\varepsilon_0}}\sqrt{\frac{2}{\varepsilon_r+1}} = \frac{v_0}{2f_r}\sqrt{\frac{2}{\varepsilon_r+1}} \qquad (1)$$

Where W is the width of the rectangular patch, m; f_r is the resonant frequency in the dominant mode, Hz; μ_0 is the vacuum permeability, H/m; ε_0 is the vacuum permeability, F/m; ε_r is the dielectric constant of the substrate; and, v_0 is the vacuum phase velocity of the light, m/s. The flux lines of the electric and magnetic fields do not remain between the patch and the ground plane, because the flux lines are curved in the edges of the patch. This problem causes an inhomogeneous media, the substrate of the PCB and air. In order to get a good approximation, it is necessary to obtain an effective dielectric constant ε_{reff} that has an intermediate numerical value in comparison with the PCB substrate and air, see equation (2).

$$\varepsilon_{reff} = \frac{\varepsilon_r+1}{2} + \frac{\varepsilon_r-1}{2}\left[1+12\frac{h}{W}\right]^{-1/2} \qquad (2)$$

Where ε_r is the dielectric constant of the substrate; and, h is the thickness of the substrate, m. The curved flux lines of the electromagnetic field introduce another problem, because the antenna behavior looks like if the length were greater. The equation (3) determines the extension of the length.

$$\frac{\Delta L}{h} = 0.412\frac{\left(\varepsilon_{reff}+0.3\right)\left(\frac{W}{h}+0.264\right)}{\left(\varepsilon_{reff}-0.258\right)\left(\frac{W}{h}+0.8\right)} \qquad (3)$$

Where ΔL is the length increment, m; and, h is the thickness of the substrate, m. Then the actual length of the patch is determined by equation (4).

$$L = \frac{1}{2f_r\sqrt{\varepsilon_{reff}}\sqrt{\mu_0\varepsilon_0}} - 2\Delta L \qquad (4)$$

Where L is the actual length of the patch, m; and L_{eff} is the effective length of the patch, m; see equation (5).

$$L_{eff} = L + 2\Delta L = \frac{\lambda}{2} \qquad (5)$$

Where λ is the wavelength in the propagation media, m. In order to optimize the power transfer, it is necessary to calculate the antenna impedance, see equations (6), (7) and (8).

$$Z_{in} = \frac{1}{Y_{in}} = R_{in} = \frac{1}{2G} \qquad (6)$$

$$G = \begin{cases} \frac{1}{90}\left(\frac{W}{\lambda_0}\right)^2, & W \ll \lambda_0 \\ \\ \frac{1}{120}\left(\frac{W}{\lambda_0}\right), & W \gg \lambda_0 \end{cases} \qquad (7)$$

$$\lambda_0 = \frac{c}{f_r} \qquad (8)$$

Where G is the patch conductance, λ_0 is the vacuum wavelength, m; and, c is the phase velocity of light in the vacuum, m/s. It is important to see that equation (7) is an asymptotic approximation. In this paper the feeding line transmission was calculated using a quarter wavelength transformer.

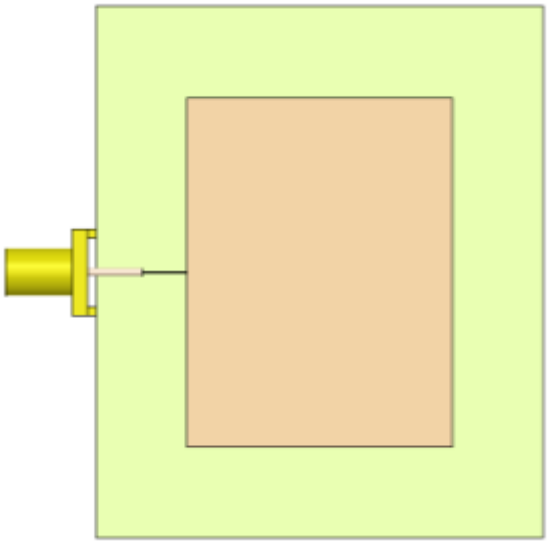

Fig.2 Rectangular patch antenna with a microstrip line transmission feed.

2.2 Antenna array and matching network design

The linear rectangular-patch antenna array has two rectangular patches and their 50 Ω transmission lines in the top layer of the PCB, where it must be placed the phase center of the array. In this case the matching network was implemented width microstrip line transmissions as is illustrated in the Fig. 2. The matching network is symmetrical because the patches have identical geometries, and it is built with a 100 Ω T-patch, two 70.71 Ω quarter wave-length transformers and a 50 Ω microstrip line transmission.

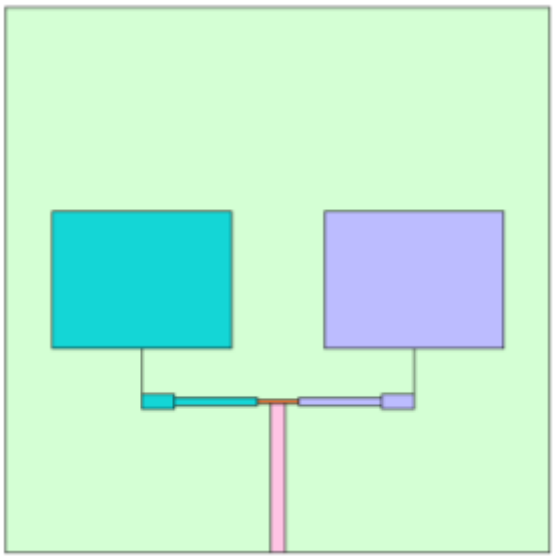

Fig.3 Rectangular patch antenna array with the matching network.

3 Problem Solution

Using the procedure described before, the resulting dimensions of the primary radiator are summarized in the Table 1 and can be shown in Fig. 4.

	[mm]	Approximation	Optimized
Width	W	38.393	38.393
Length	L	29.798	29.1
Feeder width	W_f	0.1596	0.18
Feeder length	L_f	18.667	10.0

Table 1. Rectangular patch antenna.

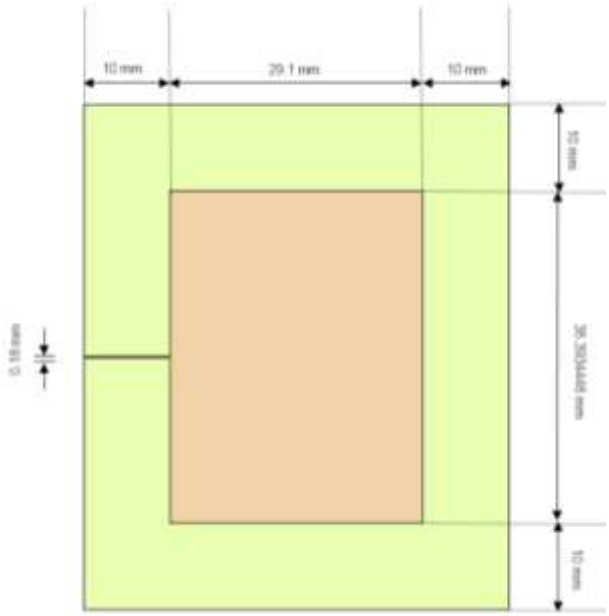

Fig.4 Rectangular patch antenna with a microstrip line transmission feed.

Employing this information, the rectangular patch radiator was simulated with the HFSS (High Frequency Structure Simulator) software package, that is a full-wave simulator based on Finite Element Method (FEM).

The initial model of this structure is illustrated in Fig. 5 in HFSS software. This model can be improved in the computation tool, because the model was calculated with empirical formulas. In fact, the numerical method in HFSS (Finite Element Method FEM) has a good approximation in this kind of antenna.

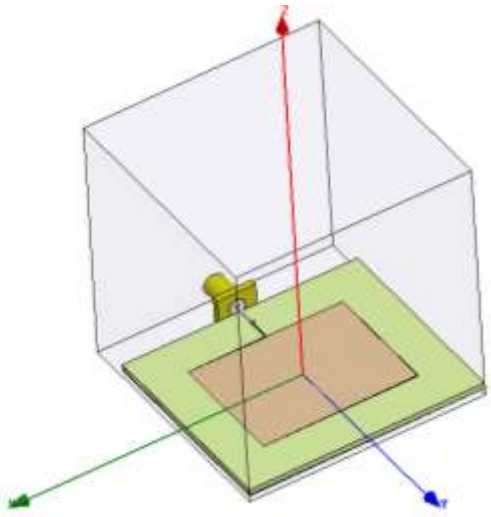

Fig.5 Model of the rectangular patch radiator.

The Fig. 6 shows the return loss of the rectangular patch after the optimization stage. In order to obtain a resonant frequency of 2.4 GHz, the optimized model was employed.

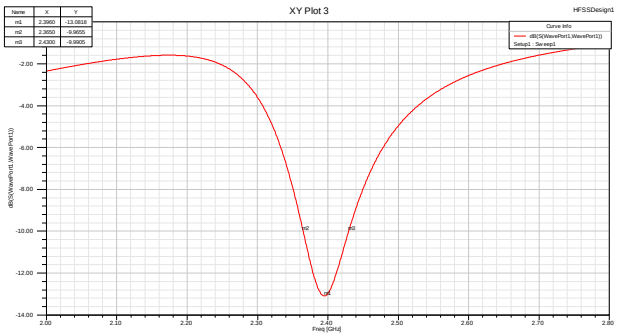

Fig.6 S_{11} parameter of the optimized model of the rectangular patch.

The performance of the radiator in the space is completed with the 3D and polar antenna patters that are illustrated of the Fig. 7 and Fig.8, respectively.

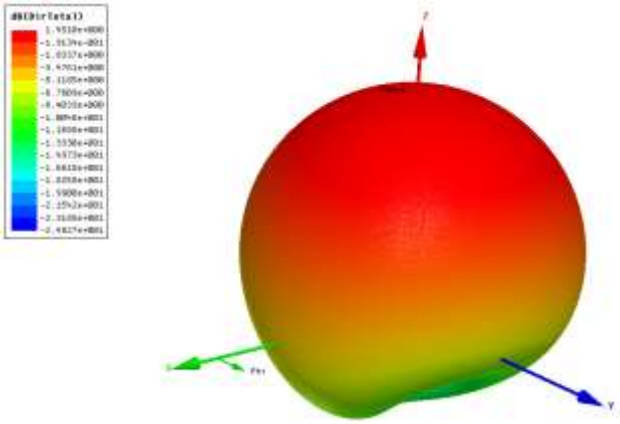

Fig.7 3D radiation pattern of the optimized model of the rectangular patch.

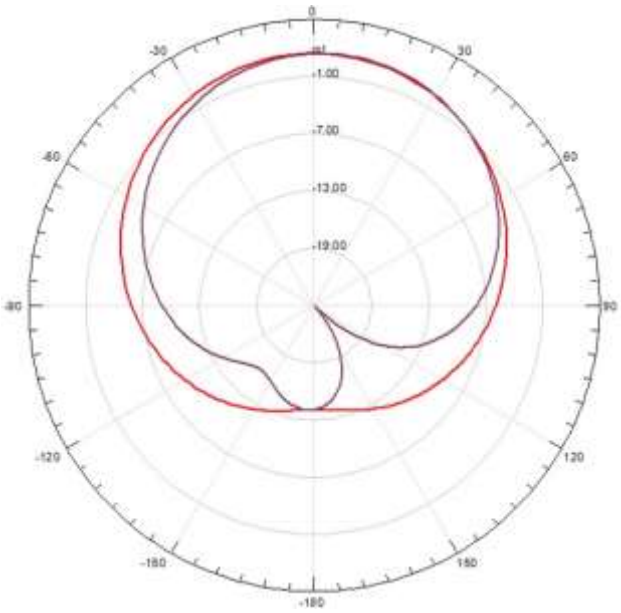

Fig.8 Polar antenna pattern of the optimized model of the rectangular patch.

The primary radiator was built using optical and chemical techniques. The optimized model in HFSS was exported and printed, see Fig. 9.

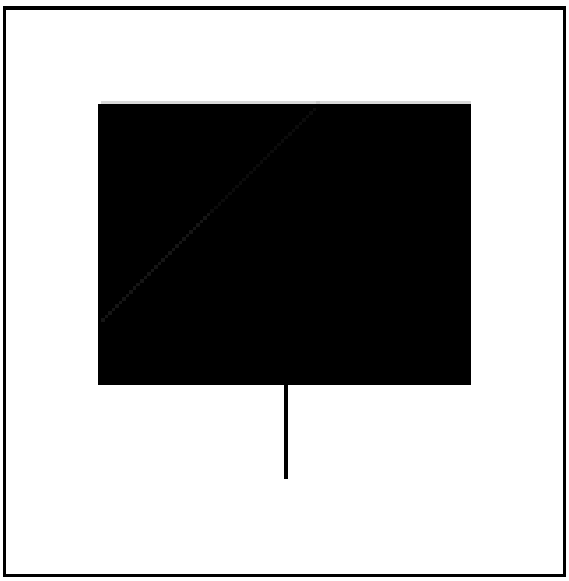

Fig.9 Exported file used in primary radiator fabrication.

The primary radiator was built using optical and chemical techniques. The optimized model in HFSS was exported and printed, see Fig. 9. The single radiator built with optical and chemical methods is illustrated in the Fig. 10.

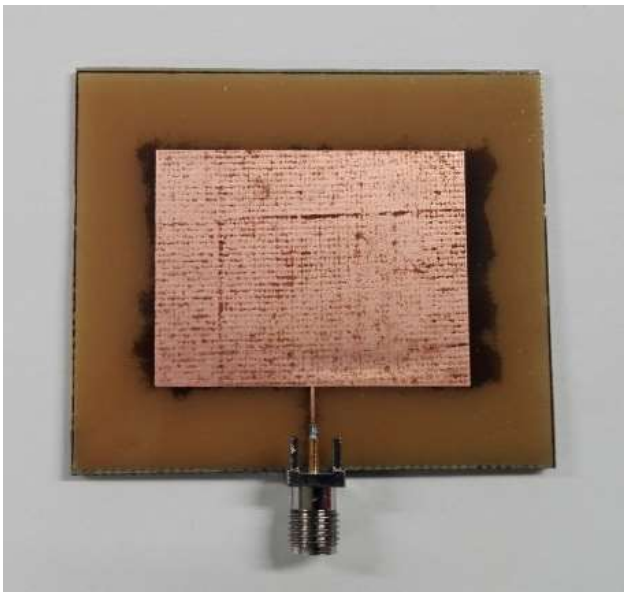

Fig.10 Single radiator of the array.

The rectangular patch radiator was measured using a near-field scanner (RFX RFxpert by EMSCAN) and a network analyzer. This kind of equipment computes a far-field antenna pattern by interpolation of the near field detected with a set of sensors placed below the scanner surface. The scanner is compatible with planar microstrip antennas, and it is necessary to place the bottom layer of the PCB over the scanner, see Fig. 11 and Fig.12.

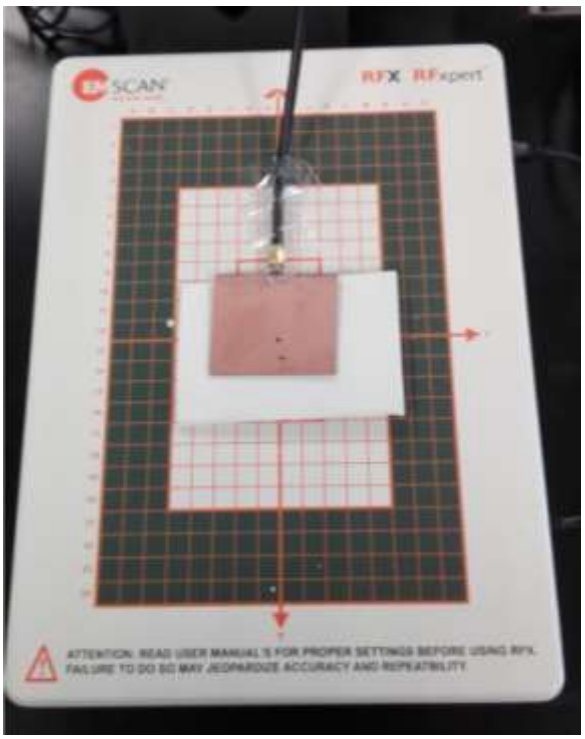

Fig.11 Single radiator measurement using a near-field scanner.

Fig.12 Near-field measurement in progress with the single-radiator.

The main results obtained with the Network Analyzer (NA), a Personal Computer (PC) and the near field scanner can be appreciated in Fig. 13. The software of the scanner shows the far field obtained by interpolation, see Fig. 14. The PC uses the ethernet port to control the NA and the near-field scanner.

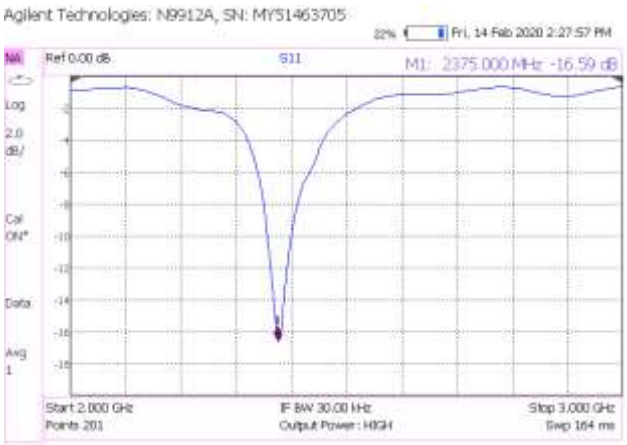

Fig.13 Experimental result of S_{11} parameter for the single-patch radiator.

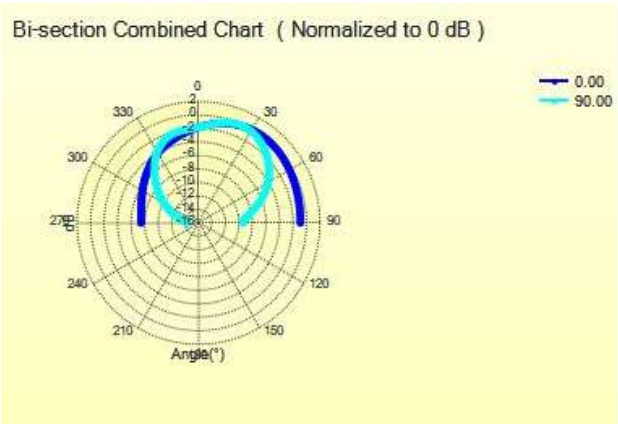

Fig.14 Radiation pattern of the primary patch.

Using the design procedure that was described in the Section 2, the main features of the antenna array is presented in Table 2. The initial model of the antenna array that was used in the HFSS simulation is presented in Fig. 15.

	[mm]	Initial	Optimized
Patch width	W	38.3934	38.3934
Patch length	L	29.1	29.1
Left patch width	W_{f1}	0.18	0.18
Right patch length	L_{f1}	10.0	10.0
50 Ω Tx line width	W_{f2}	3.0029	2.9756
50 Ω Tx line length	L_{f2}	17.2913	7.0
70.71 Ω Tx line width	W_{f3}	1.5969	1.5595
70.71 Ω Tx line length	L_{f3}	17.7066	17.7499
100 Ω Tx line width	W_{f4}	0.70325	0.6672
100 Ω Tx line length	L_{f4}	18.1467	9.07364
50 Ω main Tx line width	W_{f5}	3.0029	2.97561
50 Ω main Tx line length	L_{f5}	17.2913	32.0220

Table 2. Main features of the antenna array.

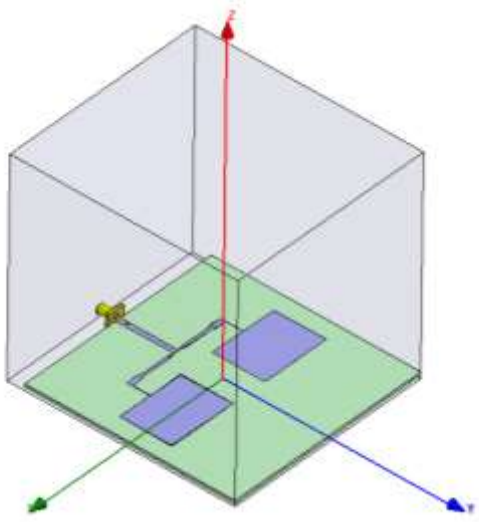

Fig.15 Initial model of the antenna array.

The return loss of the optimized model of the antenna array are plotted in Fig. 16, where the S_{11} is used in logarithmic scale.

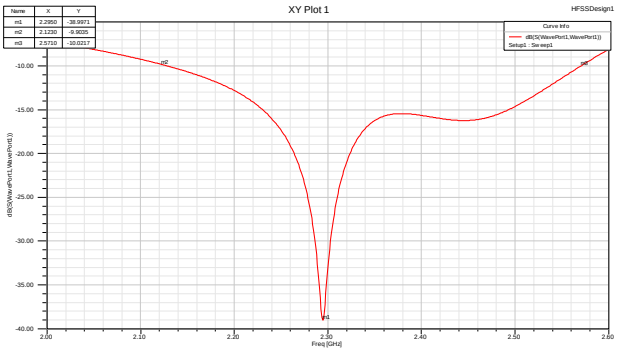

Fig.16 S_{11} parameter of the antenna array obtained by simulation.

The antenna patterns of the optimized model of the antenna array are shown in Fig. 17 and 8, for both tri-dimensional and polar diagrams, respectively.

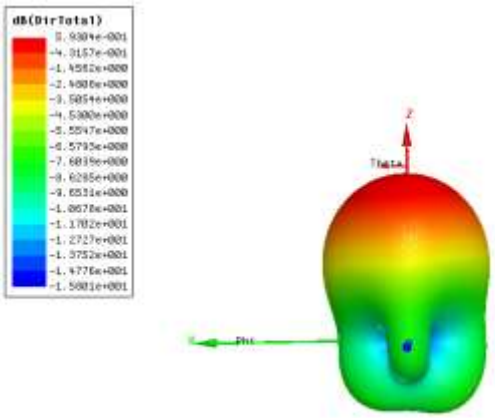

Fig.17 3D antenna pattern of the array.

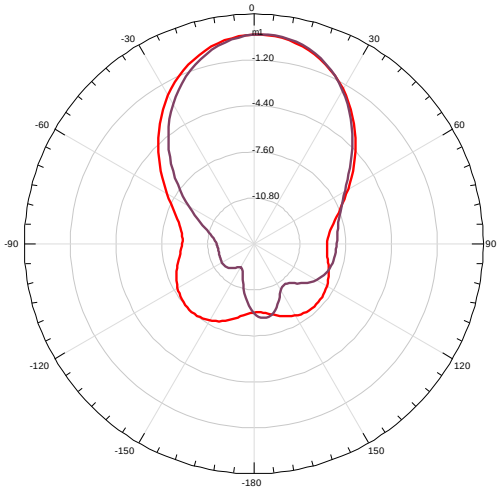

Fig.18 Polar antenna pattern of the optimized antenna array.

The antenna array was fabricated using the printing file that is shown in Fig. 19. This file was exported from HFSS in DXF format, which is one of the most compatible AUTOCAD files.

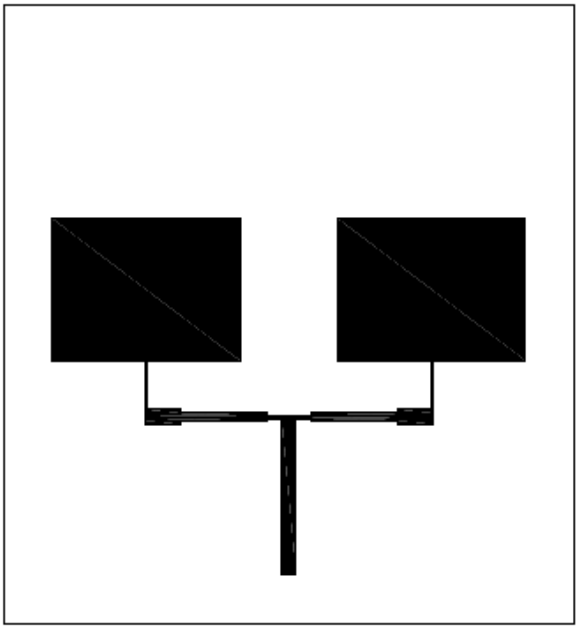

Fig.19 HFSS exported file used in the array.

The antenna array was built using very well-known optical and chemical methods. The final appearance of the antenna array can be seen in the Fig. 20.

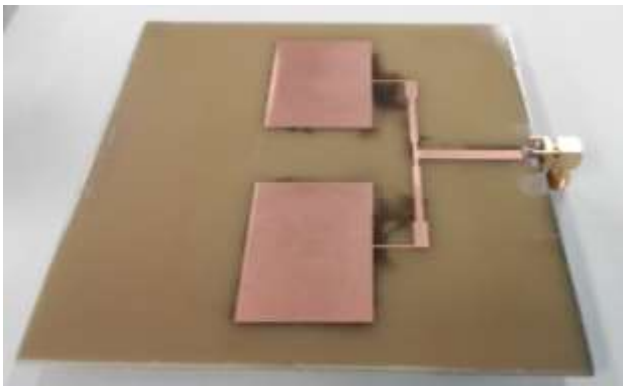

Fig.20 Antenna array that was built and evaluated by experimental methods.

Employing the same approach that was used in the single-radiator, antenna array was evaluated by near-field measurement. The EMSCAN scanner was controlled using ethernet ports from a PC, see the Figure 21.

Fig.21 EMSCAN Scanner configuration used in the measurement of the antenna array.

The far-field interpolation calculated by the EMSCAN is illustrated in the Fig.22 and 23, where tridimensional and polar antenna diagrams were plotted.

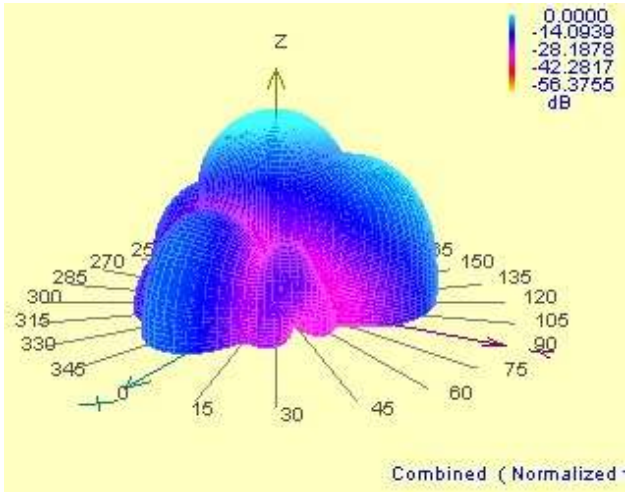

Fig.22 Tri-dimensional antenna pattern obtained using the EMSCAN scanner.

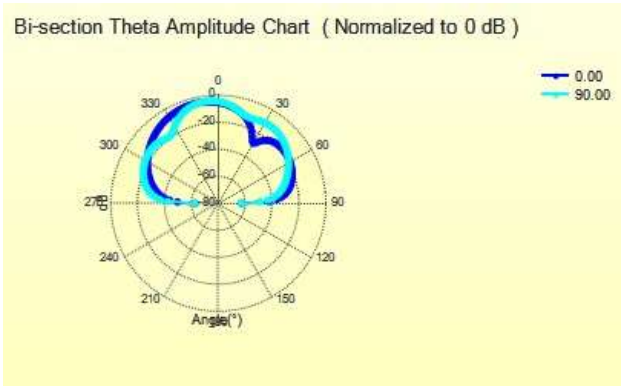

Fig.23 Polar antenna pattern obtained using the EMSCAN scanner.

Finally, the return loss of the rectangular-patch antenna array was obtained using the FieldFox Network Analyzer, see the Fig.24.

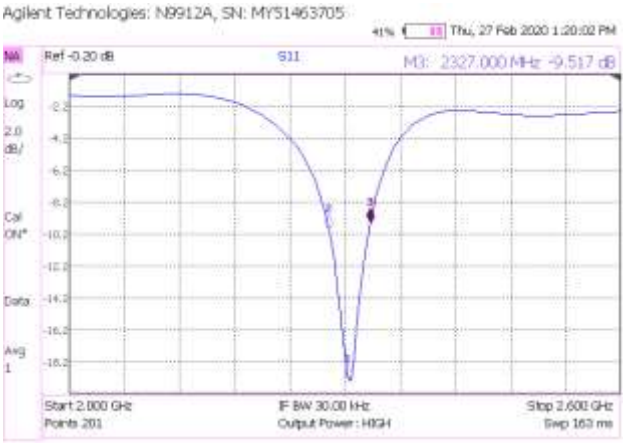

Fig.24 S_{11} parameter obtained using the EMSCAN scanner.

A comparison of simulation and experimental results is shown in Table 3, where HFSS row is related to the optimized model of the antenna array.

	Resonant Frequency [GHz]	Bandwidth [%]
HFSS	2.3960	2.7128
FieldFox RF Analyzer	2.3750	1.8947

Table 3. Comparison of simulation and experimental results.

4 Conclusion

A 2x1 rectangular patch antenna array was designed, simulated, optimized, built and evaluated, for 2.4 GHz band application. This antenna is already used in radiocommunication undergraduate courses at Metropolitan Autonomous University. The antenna was designed in order to be built using low-cost materials and techniques, like optical and chemical methods. The PCB selected for the antenna is the FR-4 substrate with a thickness around 1.544 mm. The HFSS software package was used in the simulation and optimization procedures. The antenna array it is now improved with weighting factor in the single-radiator elements of the array, with the aim to identify the source direction in a 2-D coverage area structures [12], [13], [19].

Experimental and simulation results are quite similar, where narrowband feature is obvious, due of usage of rectangular patches in the single radiator role structures [14], [15], [17].

At this time a software is in construction in order to obtain a computational tool to compute the antenna layouts, including the matching network. It is possible to improve the antenna arrays if the matching network uses a LCR circuits, because the radiation efficiency normally is reduced with microstrip transmission lines. The features of the single radiator can be increased using a broadband or multi-band defected [16], [18], [20],[21]. Besides the work presented here is the first stage of a set of antennas in spatial discrimination with some kinds of apertures [22], [23].

References:

[1] C. A. Balanis, Antenna Theory, 3rd Edition, New Jersey, John Wiley & Sons, 2016.

[2] J. L. Volakis, Antenna Engineering Handbook, McGraw-Hill, 5th Edition, 2019.

[3] D. M. Pozar, Microwave Engineering, 4th Edition, New Jersey, John Wiley & Sons, 2012.

[4] G. Ramesh, P. Bhartia, I. J. Bahl, A, Ittipiboon, Microstrip Antenna Design Handbook, Norwood MA, USA, Artech House Publishers, 2001.

[5] R. E. Munson, Conformal Microstrip Antennas and Microstrip Phased Arrays, *IEEE Transactions on Antennas and Propagation*, Vol. AP-22, No. 1, January, 1974, pp. 74 – 78.

[6] J. Q. Howell, Microstrip Antennas, *IEEE Transactions on Antennas and Propagation*, Vol. AP-23, No. 1, January, 1975, pp. 90 – 93.

[7] D. S. Chang, Analytical Theory of an Unloaded Rectangular Microstrip Patch, *IEEE Transactions on Antennas and Propagation*, Vol. AP-29, No. 1, January, 1981, pp. 54 – 62.

[8] J. R. James, P. S. Hall, C. Wood, A. Henderson, Some Recent Developments in Microstrip Antenna Design, *IEEE Transactions on Antennas and Propagation*, Vol. AP-29, No. 1, January, 1981, pp. 124 – 128.

[9] W. F. Richards, Y. T. Lo, D. D. Harrison, "An Improved Theory for Microstrip Antennas and Applications, *IEEE Transactions on Antennas and Propagation*, Vol. AP-29, No. 1, January, 1981, pp. 38 – 46.

[10] S. S. Hong, Y. T. Lo, Single-Element Rectangular Microstrip Antenna for Dual-Frequency Operation, *Electronics Letters*, Vol. 19, No. 8, August, 1983, pp. 298 – 300.

[11] H. Pues and A. Van de Capelle, Accurate Transmission-Line Model for the Rectangular Microstrip Antenna, *IEE Proceedings*, Vol. 131, No. 6, December, 1984, pp. 334 – 340.

[12] D. M. Pozar, An Update on Microstrip Antenna Theory and Design Including Some Novel Feeding Techniques, *IEEE Transactions on Antennas and Propagation Society Newsletter*, Vol. 28, October, 1986, pp. 5 – 9.

[13] T. Huyn, K. F. Lee, Single Layer Single Patch Wideband Microstrip Antenna, *Electronics Letters*, Vol. 31, No. 16, August, 1995, pp. 1310 – 1312.

[14] S. Liu, S. S. Qi, W. Wu, D. G. Fang, Single-Layer Single-Patch Four-Band Asymmetrical U-Slot Patch Antenna, *IEEE Transactions on Antennas and Propagation*, Vol. 62, No. 9, September 2014, pp. 4895 – 4899.

[15] E. F. Kuester, D. Chang, A Geometrical Theory for the Resonant Frequencies and Q-Factors of Some Triangular Microstrip Patch Antennas, *IEEE Transactions on Antennas and Propagation*, Vol. AP-31, No. 1, January, 1983, pp. 27 – 34.

[16] J. S. Dahele, K. F. Lee, Theoretical and Experimental Studies of the Resonant Frequencies of the Equilateral Triangular Microstrip Antenna, *IEEE Transactions on Antennas and Propagation*, Vol. 40, No. 10, October, 1992, pp. 1253-1256.

[17] N. Kumprasert, W. Kiranon, Simple and Accurate Formula for the Resonant Frequency of the equilateral Triangular Microstrip Patch Antenna, *IEEE Transactions on Antennas and Propagation*, Vol. 42, No. 8, August, 1994, pp. 1178 - 1179.

[18] S. C. Pan, K. L. Wong, Dual-Frequency Triangular Microstrip Antenna with a Shorting Pin, *IEEE Transactions on Antennas and Propagation*, Vol. 45, No. 12, April, 1997, pp. 1889 - 1891.

[19] E. G. Lim, E. Korolkiewicz, S. Scott, A. Sambell, B. Aljibouri, An Efficient Formula for the Input Impedance of a Microstrip Right-Angled Isosceles Triangular Patch Antenna, *IEEE Antennas and Wireless Propagation Letters*, Vol. 1, 2002, pp. 18 - 21.

[20] J. H. L, C. L. Tang, K. L. Wong, Single-Feed Slotted Equilateral-Triangular Microstrip Antenna for Circular Polarization, *IEEE Antennas and Wireless Propagation Letters*, Vol. 47, No. 7, July 1999, pp. 1174 - 1178.

[21] D. Guha, J. Y. Siddiqui, Resonant Frequency of Equilateral Microstrip Antenna With and Without Air Gap, *IEEE Transactions on Antennas and Propagation*, Vol. 52, No. 8, August, 2004, pp. 2174 - 2177.

[22] C. Guo, J. Li, D. Yang, H. Zhai, Compact Co-Polarized Decoupled Microstrip Patch Array Antenna Based on TM02/TM03 Modes Cancellation, *IEEE Transactions on Antennas and Propagation*, Vol. 70, No. 10, October, 2022.

[23] S. Qi, J. J. Zhao, W. Wu, Ka-Band Single-Layer High-Efficiency Circular Aperture Microstrip Array Antenna, Hindawi, International Journal of Antennas and Propagation, Vol. 2022, 2022.

Contribution of Individual Authors to the Creation of a Scientific Article (Ghostwriting Policy)

Jeanette Mejia Rojas	Formal analysis, investigation, methodology, writing – original draft
Mario Reyes-Ayala	Conceptualization, investigation formal analysis, writing, review and editing
Edgar Alejandro Andrade-Gonzalez	Project administration, resources, review, validation
Sandra Chavez-Sanchez	Visualization, review validation
Hilario Terres-Peña	Supervision, validation, review
Rene Rodriguez-Rivera	Validation, review

Sources of Funding for Research Presented in a Scientific Article or Scientific Article Itself

This work was supported by the research project EL002-18 in the Metropolitan Autonomous University in Mexico City.

Conflicts of Interest

The authors have no conflicts of interest to declare that are relevant to the content of this article.